



**HAL**  
open science

# Comparing Various Methods for Topology and Shape Optimization of Floating Breakwaters

Ghassan Elchahal, Pascal Lafon, Rafic Younes

► **To cite this version:**

Ghassan Elchahal, Pascal Lafon, Rafic Younes. Comparing Various Methods for Topology and Shape Optimization of Floating Breakwaters. WSEAS Transactions on Fluid Mechanics, 2008. hal-03610989

**HAL Id: hal-03610989**

**<https://hal.science/hal-03610989v1>**

Submitted on 22 Mar 2022

**HAL** is a multi-disciplinary open access archive for the deposit and dissemination of scientific research documents, whether they are published or not. The documents may come from teaching and research institutions in France or abroad, or from public or private research centers.

L'archive ouverte pluridisciplinaire **HAL**, est destinée au dépôt et à la diffusion de documents scientifiques de niveau recherche, publiés ou non, émanant des établissements d'enseignement et de recherche français ou étrangers, des laboratoires publics ou privés.

## Comparing Various Methods for Topology and Shape Optimization of Floating Breakwaters

GHASSAN ELCHAHAL

Charles Delaunay Institute,  
Mechanical System and Concurrent  
Engineering Laboratory FRE CNRS  
University of Technology of Troyes-  
FRANCE

ghassan.el\_chahal@utt.fr

PASCAL LAFON

Charles Delaunay Institute,  
Mechanical System and Concurrent  
Engineering Laboratory FRE CNRS  
University of Technology of Troyes-  
FRANCE

pascal.lafon@utt.fr

RAFIC YOUNES

3M Mechanical Laboratory  
of Engineering  
Lebanese University –  
Faculty of Engineering  
LEBANON

ryounes@ul.edu.lb

*Abstract:* In this paper, structural optimization of a floating breakwater is addressed through several methods concerning its topology and shape, which constitutes a new application. Three methods are introduced to handle the optimization problem. The first one discusses the shape optimization of a simple predefined geometrical form. The second, studies the topological optimization based on bit array representation of a triangular mesh using genetic algorithms. An attempt to overcome the limitations of bit-array was developed through several steps (new partition element, mesh distinguishing between the representation type and finite element analysis, varying finite element problem size, creating a density vector to control the presence or absence of the boundaries, generating initial population representing void domains instead of void elements). The third method concerns shape optimization, based on a variable number of points creating a structural domain. In contrary to traditional methods where the variable points are indicated by the user, it searches for the optimum number of points to create the optimum shape. Finally, a comparison between these methods for the case of the floating breakwater is discussed.

*Keywords:* Wave modelling; Floating breakwaters; Shape and topology optimization.

### 1 Introduction

Floating breakwaters present an alternative solution to conventional fixed breakwaters and can be effectively used in coastal areas with mild wave environment conditions. Poor foundation or deep-water conditions as well as environmental requirements, such as phenomena of intense shore erosion, water quality and aesthetic considerations advocate the application of such structures. They have many advantages compared to the fixed ones, e.g. absence of negative environmental impacts, flexibility of future extensions, mobility and relocation ability, lower cost and ability of a short time transportation and installation. As a result of all these positive effects, many types of floating breakwaters have been developed. However, the most commonly used type of floating breakwaters is the one that consists of rectangular pontoons connected to each other and moored to the sea bottom with cables. Moreover, many studies have been developed and mainly concerning the wave

protection improvement by different types of floating structures and their performance. Other studies have been directed towards mooring forces and motion responses to understand their behaviour due to sea waves. For example, [4] presented a simplified analytical model for a floating rectangular breakwater in water of finite depth. Williams [20] analyzed the Froude–Krylov force coefficients for the case when a rectangular body is located close to the free surface or sea bed. Williams and Abul-azm [21] studied the case of a dual pontoon floating breakwater and investigated the effects of the various wave and structural parameters on the efficiency of a dual breakwater. Williams et al. [22] investigated the hydrodynamic properties of a pair of long floating pontoon breakwaters of rectangular section. Lee and cho [11] developed a numerical analysis using the element free Galerkin method and mainly concerning the influence of mooring line condition on the performance of FBWs. Shen et al [15] studied the effects of the

bottom sill or simply changing the topography on the hydrodynamic and transmission coefficients by a semi analytical method. Loukogeorgaki and Angelides [12] focused on a three dimensional modelling of the floating body coupled with a static and dynamic model of the mooring lines. Gesraha [8] investigated the reflection and transmission of incident waves interacting with long rectangular floating breakwater with two thin sideboards protruding vertically downward, having the shape of the Greek letter  $\Pi$ .

From the researches of the scholars above, we find most of them focus attention on the modelling of floating breakwaters. Yet none of these studies have been discussing the structural design of floating breakwaters or more even its optimization. On the other side, optimization of fixed breakwaters has been previously discussed in [13] but focused on minimizing the cost function imposed to structural failure constraints. Also, we have elaborated a previous optimization problem but for a floating breakwater based on analytical modelling with a simple static approach, which really imposed many restrictions on the modelling and optimization of the entire problem [5]. Therefore, in this paper the study is directed towards optimization of floating breakwaters to reduce its weight, or to represent a new resistive form, in accordance to the physical and mechanical constraints. The modelling procedure in this paper is traditional where an optimization problem is studied for a new application. Thus, it is necessary to apply various methods for this new application, in order to compare them and choose the most efficient to be applied later on sophisticated wave-structure interaction models. Moreover, there are new contributions in the applied methods which had really been very utile in this practical problem.

The first method concerns the optimization with a predefined rectangular geometrical shape based on the Sequential Quadratic programming method (SQP), which constitutes a direct approach in the optimization world. The second, concerns topology optimization based on bit-array using genetic algorithms; with a new mass representation type, triangular form, based on an elementary mesh (Delaunay triangulation). The bit-array representation has been widely adopted ([14], [10], [16], [6], [8], [3], [19]). In spite of its success in solving topology optimization design problems, bit-array representation suffers from a strong limitation due numerous reasons: dependency of its complexity on that of the underlying mesh, fixed

rectangular finite element mesh, connectivity, and initial population generation. The only attempt to overcome mesh dependency, the most serious obstacle, between the partition of the design and domain and the FE computations was introduced by Schoenauer and his co-workers [14],[8]) through the voronoi diagrams. But, these voronoi diagrams have undesired shapes that surely affect the topology representation of the optimal solution. They are useful structures encountered in several disciplines and mainly appearing in the study of crystal growth or in studies on the great structures of the universe.

Although the Voronoi and the Delaunay triangulations are completely determined by each other, there exists a significant difference. Whereas the Voronoi may differ topologically (i.e., they may have different numbers of faces and edges), the Delaunay are always topologically equivalent. The Voronoi diagram is a division of the plane into polygons with different sizes and number of edges. Where, a Delaunay triangulation minimizes the maximum interior angles, providing the most "equable" triangulation of a given set of points. Moreover, Delaunay triangulation minimizes the distance between all surface points and nodes, which results in a highly accurate surface representation. Therefore, the triangular partition will surely yields to more accurate and representable shapes when compared to voronoi. This will appear clearly when treating optimization problems that demands symmetric repartition (floating structures), which is very difficult to obtain with the voronoi due to their irregular shapes. On the other side, the triangular mesh is also much better than the particular rectangular mesh, used in traditional bitarray representation, in discretizing complicated and non rectangular geometries [1].

The efficiency of different methods can be measured by the total number of FE based evaluations required in reaching those optimal results since the FE analysis is the most consuming part of the procedures. Generally, the bit-array and the voronoi diagrams are mapped into the two dimensional design domain discretized by a fixed regular mesh; where the choice of the mesh size is considered in accordance to reduce the computational cost. The second important idea in the present topology algorithm is the varying number of FE equations for each individual in during optimization, yielding to an effective reduction in the entire consumable time. This appears also in conjunction with this triangular partition, where the density (mass) distribution is

defined through a second algorithm that creates a new geometrical domain (excluding all the void elements). Then a refined mesh is generated on this new domain which is completely different from the one used in the design domain partition. Thus, we solve in each iteration the appropriate number of FE equations relevant to the topology of each individual. Where all the others ([19], [3], [8], [6], [10], [16], [14]) solve the FE computations on the whole design domain due to a fixed finite element mesh that does not change its size whatever is the topology (a small Young's modulus is assumed for void elements). Therefore, we can use very fine meshes without affecting the size of the optimization problem.

Another important contribution is the initialization of the topology problem or simply the generation of the initial population. All the previous topology problems are randomly initialized except for the case of [17] and [19] that proposed identical individuals in the initial population, where the whole design domain is filled with material. In this study we initialize admissible or physical domains instead of void elements, and this surely speeds up the convergence of the problem.

The third method in our paper concerns shape optimization by using an optimum number of variable points which create an arbitrary valid domain, based on the SQP method. The coordinates of these points represent the variables for the optimization problem. The novelty of this work appears in searching for the optimal number of points needed to describe the optimal shape. Previous methods ([2], [18]) select key points from existing geometries or some nodal points deduced from the meshing procedure of this existing geometry to constitute the design variables of the optimization. But all of these studies are based on the designer selection. In this paper, the goal is not only to obtain the optimum shape by varying the coordinates of the points, but also to obtain the optimum shape by the optimal number of points. In optimization problems addressing the interior boundaries, it will be very efficient to generalize the problem instead of indicating a definite shape (rectangle, circle, ellipse,..). Thus, it is very useful to vary the number of points yielding to a new shape. Finally, a comparison between these methods is performed to reveal various methods for our new application problem.

The methodology followed in this paper starts by identifying an analytical modelling of waves and their induced pressures. Second, the optimization

problem is defined by introducing the objective function and the imposed constraints in a general form. After this, the latter are expressed in accordance to the representation type of each optimization method. Finally, a practical application with Matlab is developed. It is interesting to consider the case of a breakwater appearing in ports' far from the shore, at a constant depth. Then, the problems of waves propagation over a varying bathymetry and shallow water consequences are eliminated.

## 2-Wave Modelling

A cartesian coordinate system  $Oxyz$  is employed, where  $Oxy$  coincide with plane of the free surface at rest,  $Oz$  directed positive upwards, and  $Ox$  directed positive in the direction of propagation of the waves. The incident wave propagates in a straight line in the direction of  $Ox$  axe to obtain the maximum pressure applied by the waves on the breakwater (incident wave normal to the breakwater) and the movement is reduced to two dimensions (Figure 1). The fluid motion is defined as follows: Let  $t$  denote time,  $x$  and  $z$  the horizontal and vertical coordinates,  $\eta$  the free-surface elevation above the still water level, and  $\Phi$  the velocity potential. The characteristic parameters of the wave are defined in (Fig.1).

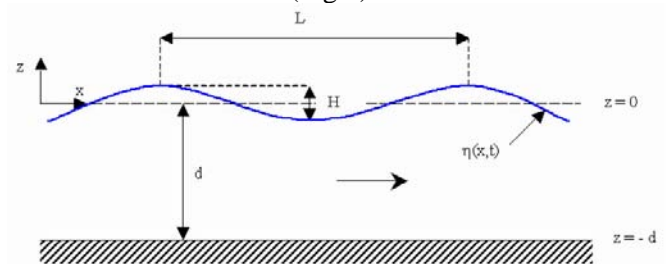


Figure 1 Wave notations

The boundary value problem is then defined by:

$$\nabla^2 \Phi = \Delta \Phi = 0 \quad \text{Laplace equation} \quad (1)$$

$$\left( \frac{\partial \Phi}{\partial z} \right)_{z=-d} = 0 \quad \text{Condition at the sea floor;} \quad (2)$$

$$\left( \frac{\partial \Phi}{\partial n} \right)_{x=0} = 0 \quad \text{Kinematic condition at the solid boundary;} \quad (3)$$

$$\left( \frac{\partial \eta}{\partial t} + \frac{\partial \Phi}{\partial x} \frac{\partial \eta}{\partial x} - \frac{\partial \Phi}{\partial z} \right)_{z=\eta} = 0 \quad \text{Kinematic condition at the free surface;} \quad (4)$$

$$\left( \frac{\partial \Phi}{\partial t} + \frac{1}{2} \left( \left( \frac{\partial \Phi}{\partial x} \right)^2 + \left( \frac{\partial \Phi}{\partial z} \right)^2 \right) + g\eta \right)_{z=\eta} = Q(t)$$

Dynamic equation at the free surface. (5)

Applying the nonlinear theory (Stokes 2<sup>nd</sup> order expansion), based on the perturbation method; the expression of the pressure distribution in the case of wave-breakwater interaction, where all the waves are reflected by the breakwater is given as [5]:

$$P = a \cosh k(z+d) + b \cosh 2k(z+d) + f \quad (6)$$

$$a = \frac{\rho_e g H (r+1)}{2 \cosh kd} \cos(\omega t)$$

$$b = \frac{\rho_e g \pi H^2}{4Lsh2kd} \left[ \frac{(3r^2 + 3r + 3) \cos(2\omega t)}{sh^2 kd} - r - 1 \right]$$

$$f = \frac{\rho_e g \pi H^2}{4Lsh2kd} \left[ (-r^2 - r - 1) \cos(2\omega t) + r + 1 \right] + \rho_e H^2 \omega^2 r \cos(2\omega t)$$

(Where  $k = 2\pi / L$  designates the wave number,  $\omega$  the frequency,  $r$  the reflection coefficient,  $t$  the time,  $d$  the water depth,  $H$  the wave height,  $L$  the wave length, and  $\rho_e$  the sea water density). This hydrodynamic pressure is acting on the exterior surface of the breakwater (ocean side). It is reduced to an equation with hyperbolic functions of  $z$  (altitude), where the other variables independent of the altitude are collected together in the terms  $a$ ,  $b$ , and  $f$ .

### 3-Optimization Problem

In this model, the dynamic movement of the floating breakwater is assumed to be small. It is predicated on the fact that it is sufficient to prevent the floating breakwater from acting as a wavemaker, so that the displacements are reasonably small relative to the wave height. Another assumption is that the waves are totally reflected by the floating breakwater and its fixed seawall (water between the breakwater lower side and the bottom) and no transmitted waves are propagating inside the port. This assumption is considered a reasonable approximation for the case of small motion.

A moored floating breakwater should be properly designed in order to ensure effective reduction of the transmitted energy and, therefore, adequate protection of the area behind the floating system. This reduction is achieved by the floating

breakwater itself due to a considerable depth and by the fixed seawall concept under the breakwater for the rest underwater region. Moreover, for a breakwater to float, it is obviously designed with a hollow form to reduce the total weight of the structure.

Then, the optimisation problem is assumed to be finite dimensional constrained minimization problem, which is symbolically expressed as:

Find a design variable vector  $x$  ;  
to minimize the weight function  $f_{ob}(x)$   
subjected to the  $n$  constraints  $C_i(x) \leq 0, i=1, \dots, n$

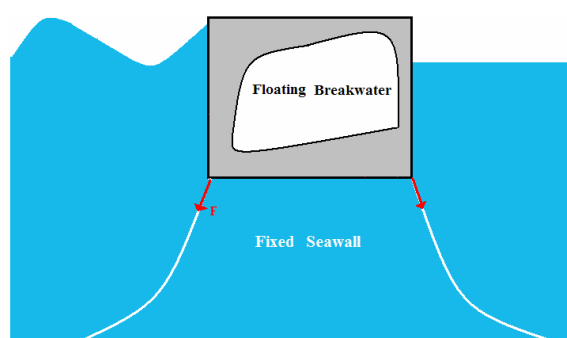


Figure 2 Characteristics of floating breakwater

### 3.1 Objective function

The optimal solution is to design a breakwater respecting all the constraints with a minimum volume, hence the objective is to minimize the weight of the breakwater.

$$f_{ob} = \min(\text{Weight}) \quad (7)$$

### 3.2 Dynamic pressure constraint

The concept of the fixed seawall permits to determine the height of the breakwater in accordance with low hydrodynamic pressure acting on this seawall. The dynamic wave pressure is mainly concentrated near the free surface and its induced perturbation is low under a certain height (Figure 3). Then the height of the breakwater can be limited to where the pressure is approximately unvarying corresponding to an approximate value of  $P - 0.1P_{max} = 0$ , where  $P_{max} = P(z=0)$ . Finally, the height can be considered to be  $L = 4m$ , where this height is indeed satisfactory for a wave with significant height ( $H = 2m$ ).

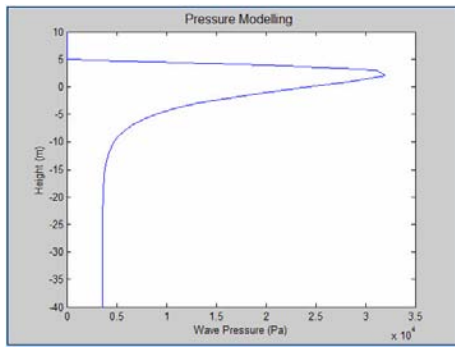


Figure 3 Wave Pressure Modelling

This constraint is independent of the other constraints, and then the height of the breakwater is determined only from it and no need to still consider the height as a variable for the rest of the optimization process.

### 3.3 Floating constraint

It is a direct application of Archimedes principle. For a moored structure, the floating constraint can be expressed in an inequality in order to minimize the weight, where the difference between the buoyancy force and the weight can be compensated by the tension in the mooring lines.

$$C_1(x) = -\rho_m V_m g + \rho_e V_T g \leq 0 \tag{8}$$

where  $\rho_m$  and  $\rho_e$  designates the densities of the material (concrete) and the sea water respectively,  $V_m$  designates the volume of the inside material of the whole breakwater, where  $V_T$  designates the volume of the submerged part of the breakwater.

### 3.4 Stability constraint

Stability is defined as the ability of the breakwater to right itself after being heeled over. This ability is achieved by developing moments that tend to restore the breakwater to its initial position. There are a number of parameters that together determine the stability of a floating breakwater.

First of all, this floating breakwater has a rectangular shape with an arbitrary core, so initially (before any disturbance) it is necessary to maintain a horizontal equilibrium position. The calculation is based on the basic formula of determining the centre of gravity (G) and then aligning it with the centre of buoyancy (B) of the floating breakwater (Figure 4) which lies at the geometric centre of volume of the displaced water ( $D/2$ ).

$x_g = \frac{\sum A_i \times x_i}{\sum A_i}$  where  $A_i$  and  $x_i$  are respectively the area and the centre of gravity of the composing geometries. Therefore, the horizontal equilibrium constraint is expressed as follows:

$$C_2(x) = x_g - \frac{D}{2} = 0 \tag{9}$$

Second, when the breakwater is disturbed by a wave, the centre of buoyancy moves from B to  $B_1$  (Figure 4) because the shape of the submerged volume is changed. Then, the weight and the buoyancy force form a couple capable to restore the breakwater to its original position. Moreover, the distance GM known as the metacentric height illustrates the fundamental law of stability, where it must be always positive to create a restoring couple and maintain stability  $\overline{GM} \geq 0$ .

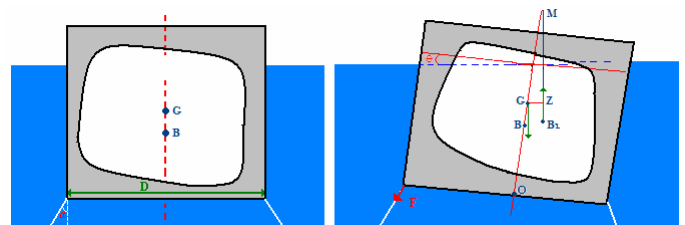


Figure 4 Stability of floating breakwater

Finally, stability is achieved by the restoring couple (weight-buoyancy) and by the tension in the mooring lines. This stability is determined around the centre of gravity, hence the moments developed by the restoring couple and the tension in cables must equilibrate the moment derived from the incoming waves.

$|Mp| - M_F - M_B = 0$ , where  $Mp$  is the moment of the disturbing force (wave),  $M_F$  is the moment of the tension in the mooring lines, and  $M_B$  is the moment of the buoyant fore (restoring couple). The absolute value of the disturbing moment guarantees the flexibility of the stability relation in the two senses of rotation. Hence, the stability constraint can be expressed by an inequality:

$$C_3(x) = -W \left( \frac{D^2}{12L} - y_g + \frac{L}{2} \right) \sin \theta - F \cos(\alpha - \theta) x_g + F \sin(\alpha - \theta) y_g + \int_{-L+y_g}^0 (a \cosh k(z+d-y_g) + b \cosh 2k(z+d-y_g) + f) z dz + \int_0^{h-y_g} (a \cosh k(z+d-y_g) + b \cosh 2k(z+d+y_g) + f) z dz \leq 0 \tag{10}$$

$h$  is the height of the breakwater portion above the still water,  $\alpha$  being the angle formed by the mooring lines and the vertical ( $\alpha=20^\circ$ ), and  $\theta$  is the angle of disturbance (heeled angle); in fact it is fixed by the designer, and since the breakwater must be very rigid and stable in order to protect the ports from waves, it is taken  $1.2^\circ$ . (slope of 2%)

### 3.5 Structural constraints

This constraint constitutes a pure structural analysis of the floating breakwater (hydrodynamic and hydrostatic pressure exerted on the surfaces), where a comprehensive numerical analysis, based on the finite element method, is requested in order to determine the mechanical stresses (Figure 5). It can be summarized by maximizing the stiffness of the structure having a given amount of mass distribution. It is well known that the concrete have different compression and traction limits due to its nature. Hence, a special criterion, named the Parabolic Criteria, [7] is introduced in terms of the principal stresses of the breakwater and the limiting stresses of the material. It can be written directly in form of an optimization constraint as follows:

$$C_4(x) = (\sigma_1 - \sigma_2)^2 - (\sigma_t + \sigma_c)(\sigma_1 + \sigma_2) - \sigma_t \sigma_c \leq 0 \quad (11)$$

where  $\sigma_1, \sigma_2$  represent the principal stresses of the structure and  $\sigma_t, \sigma_c$  represent the limiting stresses for the material constituting the examined structure. This constraint as the others must be computed in each iteration, which yields to solve the finite element problem in each iteration and for each new defined.

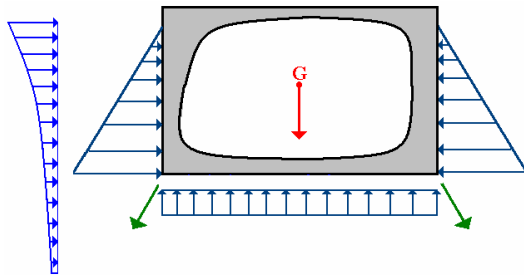


Figure 5 Floating breakwater subjected to various loads

The optimization problem defined atop, by the objective function and the related constraints, constitutes the theory of the floating breakwater optimization problem. But, what is altering is the representation type of the objective function and the relative constraints that are directly related to the optimization method itself. Therefore, the objective function (Eq.7), the floating condition (Eq.8), and the horizontal initial equilibrium condition (Eq.8)

are repeatedly symbolized in each method. Where, the stability and structural constraints (Eq.10, Eq.11) are not subjected to any change, since the first is symbolized in terms of the coordinates of the centre of gravity independent of the type of representation, and the second is purely a mechanical numerical analysis of the structure and related directly to the geometrical form ignoring the type of representation of the latter. Moreover, the problem is reduced to the optimal design of the inward domain of the floating breakwater, since the height is indicated only from the pressure constraint and then it is eliminated from the optimization problem, also the width must be fixed due to topological problems,  $D=8\text{m}$  deduced from structural constraint [5].

## 4- Shape Optimization With a Predefined Geometry

The shape optimization using a predefined geometrical form constitutes a direct approach in optimization where it can be applied only if the type of the problem permits to create a prospective image for the final shape. Hence the problem is initialized by a specific geometrical form (rectangle) and finally the optimal form will reserve the same shape but with different dimensions and location inside the outward boundary of the floating breakwater; where the variables are reduced to  $x_1, x_2, x_3, x_4$  (Figure 6).

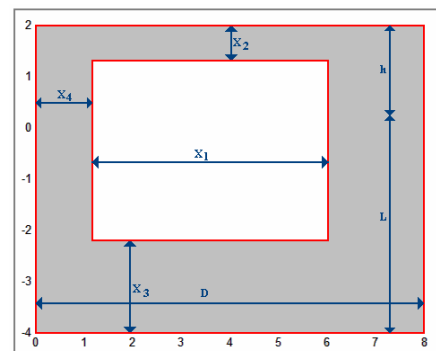


Figure 6 Predefined shape inside the floating breakwater

The height of the breakwater is divided into two parts (with respect to the calm water level): a lower part,  $L$ , deduced from the dynamic pressure constraint, and an upper part,  $h$ , equals to the height of a strong wave ( $H=2\text{m}$ ). Because, the optimization problem is dealing with a predefined geometry, then all constraints can be directly expressed in terms of the geometrical dimensions of the breakwater in form of mathematical equations.

### 4.1 Objective function

The objective function can be expressed in terms of the geometrical dimensions as:

$$f_{ob}(x_1, x_2, x_3, x_4) = \rho_m(L+h)D - \rho_m x_1(L+h-x_2-x_3)$$

### 4.2 Floating constraint

The floating constraint can be expressed as:

$$C_1(x_1, x_2, x_3, x_4) = x_1(L+h-x_2-x_3) - \frac{D(\rho_m(L+h) - \rho_e L)}{\rho_m} \leq 0$$

### 4.3 Stability constraint

The initial horizontal equilibrium and the stability of the floating breakwater depend on the calculation of the centre of gravity. This is performed by dividing the breakwater into 4 rectangles and calculating the new position of the centre of gravity (Fig. 5) in terms of the variables.

$$x_g = \frac{(L+h-x_2-x_3) \left[ \frac{(D-x_1-x_4)^2}{2} + \left(D-\frac{x_4}{2}\right)x_4 \right] + \frac{D^2}{2}[x_2+x_3]}{Dx_3 + Dx_2 + (L+h-x_2-x_3)(D-x_1)}$$

The horizontal equilibrium constraint is defined by

$$C_2(x_1, x_2, x_3, x_4) = x_g - \frac{D}{2} = 0$$

Finally, it is important to state that the expressions of the other constraints ( $C_3, C_4$ ) are conserved without changes in the three different methods, and then there will be no need for any repetition.

### 4.4 Application and results

Based on the SQP method, the numerical application yields to the following results:

$$\begin{cases} x_1 = 7.4m & x_2 = 0.367m \\ x_3 = 0.67m & x_4 = 0.3m \end{cases}$$

Replacing the variables by their corresponding values, it is capable to draw the optimized shape and its mechanical stresses distribution.

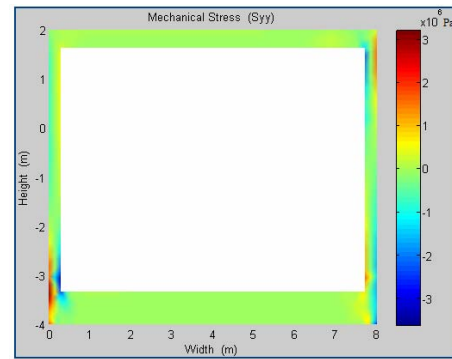
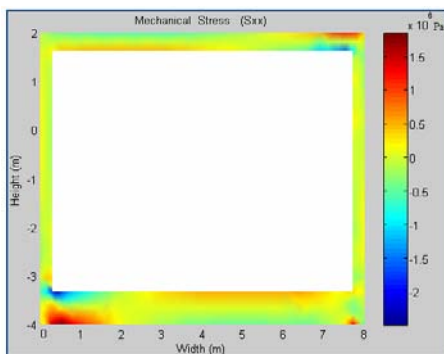


Figure 7 Mechanical stresses  $\sigma_x$  (upper) and  $\sigma_y$  (lower)

We can notice (Fig. 6) the respected limits of the mechanical stresses due to the imposed structural constraints, where the concrete has its traction and compression limits as follows:  $\sigma_t = 4MPa$ ,  $\sigma_c = -40MPa$ .

## 5- Topology Optimization

A detailed comparison between the voronoi sites and our triangular representation has been explained in the introduction. The difference between them can be clearly observed in (Figure 8).

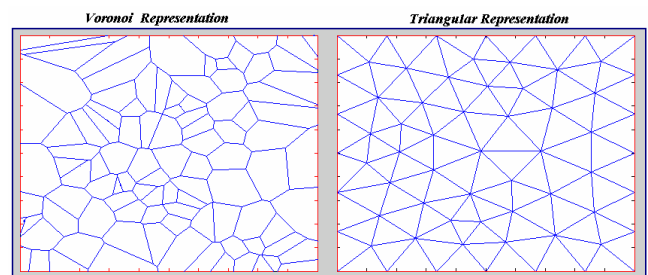
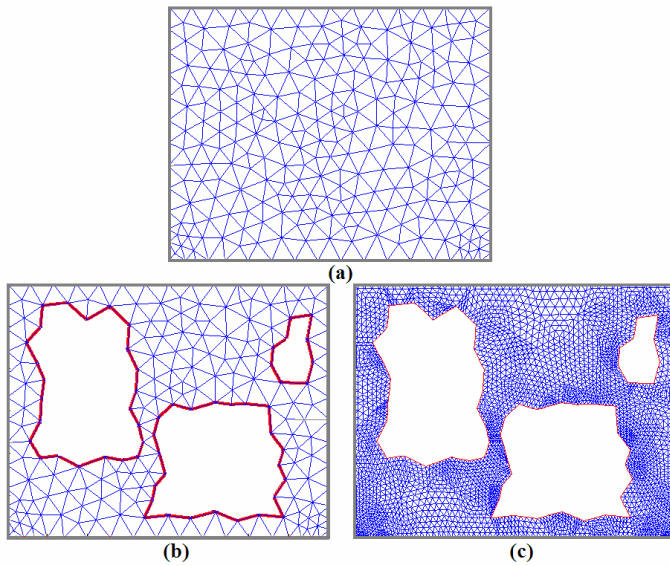


Figure 8 Voronoi and triangular representation

The objective of this topology section is to further address the bit-array representation using an elementary triangular mesh for the design domain partition (Figure 9a) and a refined triangular mesh for FE computations. In fact, this work combines the concept of the traditional bit-array representation (rectangular repartition) from the point of view of the relation between the structure itself and a regular partition, and that of the Voronoi representation in differentiating between the geometrical partition and the mesh used in FE computation. In this manner, the design domain is decomposed into approximately equable small triangles (Figure 9b) which are totally different from those of the refined mesh used in the FEM computation (Figure 9c). Therefore, the size of the FE problem is different for



each individual, where the appropriate FE problem size is solved.



**Figure 9 Different Meshes for optimisation and mechanical computation;** (a) Partition of the design domain by an elementary triangular mesh, (b) Extracting void elements from the design domain and defining a new geometrical domain, (c) Generating a refined mesh for this new geometrical domain

The geometrical properties of the mesh triangulation (nodes coordinates, edges, and triangle numbers) play an important role in simplifying the procedure of extracting or reserving specific elements in the design domain. It is easy also to escape from the problems of fine tuning of the domain boundary by reserving all the elements adjacent to the boundaries. Then, a density vector is introduced having a length equals to the total number of meshing triangles and holding only the values 0 or 1 corresponding to filled or void triangles, describing the density distribution inside the geometrical domain. This density vector establishes a relation between the geometrical identification of each triangle, its location inside the domain, and its value in the density vector. The labelling or numbering of the triangles (Figure 10) is an arbitrary process where adjacent bits in the bit string representation do not necessarily correspond to neighbour elements of the domain.

$$\rho = (\rho_1, \rho_2, \dots, \rho_n)$$

This vector undergoes a control process to confirm density distribution in specific and desirable regions (boundaries) ignoring the mutation and crossover operations through the Genetic Algorithm procedure. Thus, the optimal shape can be reached in reasonable time (especially for structures with closed boundaries) since the algorithm is able to

precisely control the boundaries of the individuals in the population.

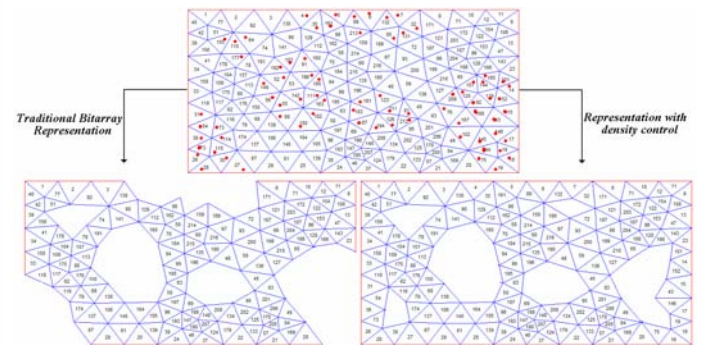


Figure 10 Representation with density control

This will definitely solve the problem of unanalyzable structures by reserving all the triangular elements adjacent to the boundary giving them the values 1 (Figure 11). Mathematically, it is expressed as follows:

$$\text{If } \begin{cases} x_{i,k} = a \\ \text{or (and)} \\ y_{i,k} = b \end{cases} \Rightarrow \rho_i = 1$$

$$\text{for } i = 1, \dots, n, \text{ and } k = 1, 2, 3$$

where  $n$  is the total number of triangles or simply it is the total number of variables in the GA,  $k$  represents the number of node in each triangle;  $x_{i,k}$  represents the  $x$  coordinates of the node  $k$  in the triangle number  $i$ ;  $y_{i,k}$  stands for the  $y$  coordinates, finally  $a$  and  $b$  stands for the boundary coordinates that needs to be conserved in all the optimization problem (they can take positive or negative values or even linear equations).

In contrary to previous methods, the initial population is generated here in a very comprehensive form. To our knowledge no one has initialized a population with admissible domains. By this way, we avoid falling in trivial solutions when the initial population is representing only arbitrary void elements. An algorithm is developed as follows:

$$\text{If } \begin{cases} h_1 < x_{i,k} < h_2 \\ \text{and} \\ h_3 < y_{i,k} < h_4 \end{cases} \Rightarrow \rho_i = 0$$

$$\text{for } i = 1, \dots, n, \text{ and } k = 1, 2, 3$$

where  $h_1, h_2, h_3, h_4$  represents correspondingly the  $x$  and  $y$  limits of this void domain. For better

performance of the GA, each individual in the initial population stands for a different representations (different  $h_1, h_2, h_3, h_4$ ).

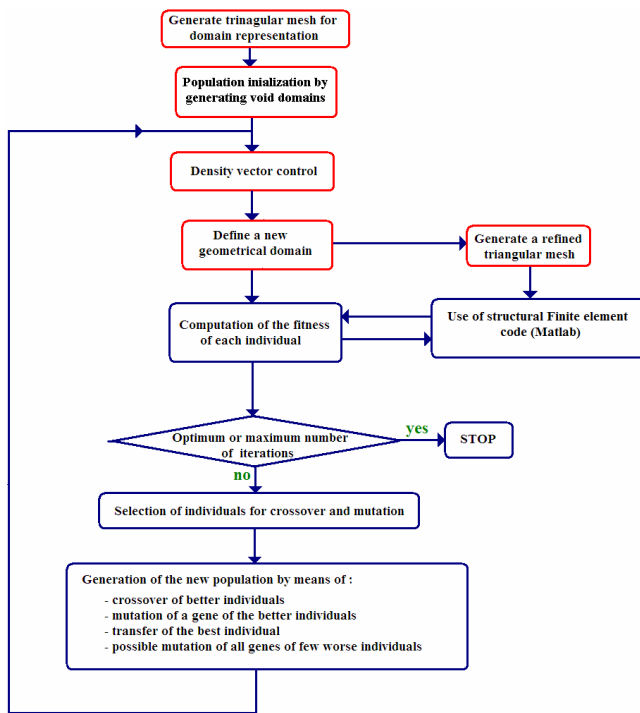


Figure 11 Flowchart for genetic algorithm

The basic algorithm of the topology optimization can be summarized in the following steps:

1-Generate an elementary triangular mesh of the design domain for structure repartition and develop the corresponding density vector. This mesh is used for mathematical computations of the relative constraints.

2-Generate an initial population composed from admissible domains. (For example see Figure 9b)

3-Density control process, where all the triangles having at least one of their nodes on any of the boundaries are marked by filled materials.

4-Define a new geometrical domain after extracting the void elements (Figure 9b). This geometrical domain varies with each individual yielding to a variable mesh size in the FE analysis. By this step we can guarantee consumable time reduction in the optimization problem.

5-Generate a refined mesh for this new structure (Figure 9c). Each individual will define a new structure, and thus the mesh size is not fixed, it varies with the structure.

6-Define the load conditions, boundary conditions, and material properties. Carry out the FE computations.

7- Computation of the fitness of the individuals.

8-If the new structural topology is not optimum, develop the crossover and mutation operations and go to step 3.

### 5.1 Objective function

Since the geometry of the structure is expressed in terms of the density distribution or mesh triangulation, the weight will be expressed in terms of the latter.

$$f_{ob}(\rho) = \rho_m \sum_{i=1}^n \rho_i \times A_i$$

where  $n$  is the number of triangles,  $\rho_i$  and  $A_i$  are the densities and areas of the corresponding triangles. The presence or absence of each triangle in the weight calculation is guaranteed by its corresponding density value in the density vector.

### 5.2 Floating constraint

Similarly, the floating constraint is expressed as: ( $S_T$  designates the submerged area of breakwater)

$$C_1(\rho) = \sum_{i=1}^n \rho_i \times A_i - S_T \frac{\rho_e}{\rho_m} \leq 0$$

### 5.3 Stability constraint

In Such problems where the geometry is taking different shapes and varying its topology in each iteration, it will be impossible to calculate the centre of gravity in the traditional or analytical methods. Benefiting from various numerical tools, the centre of gravity and area of each triangle are calculated in the whole elementary mesh triangulation domain including both filled and void triangles. Then, we multiply their product by the density vector excluding in this manner all the void triangles from the real calculation of the centre of gravity.

$$x_g = \frac{\sum_{i=1}^n \rho_i \times A_i \times x_i}{\sum_{i=1}^n \rho_i \times A_i} \quad \text{and} \quad y_g = \frac{\sum_{i=1}^n \rho_i \times A_i \times y_i}{\sum_{i=1}^n \rho_i \times A_i}$$

where  $x_i$  and  $y_i$  are the coordinates of the centre of gravity of each triangle. Then, the relevant

horizontal stability constraint ( $x_g = D/2$ ) is written as follows:

$$G_1(\rho) = \frac{\sum_{i=1}^n \rho_i \times A_i \times x_i}{\sum_{i=1}^n \rho_i \times A_i} - \frac{D}{2} = 0$$

### 5.4 Application and results

The main properties of the GA are as follows:

- Individual length = 480,  $\rho = (\rho_1, \dots, \rho_{480})$
- Population type: Bit String
- Crossover fraction: 0.5
- Mutation: Adaptive feasible
- Crossover: Scattered

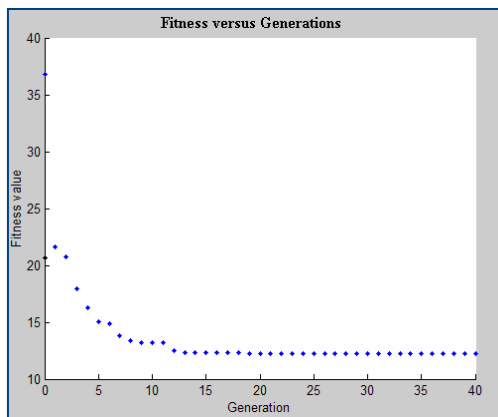


Figure 12 Fitness function versus number of generations

By this formulation we can reproduce half of the individuals by mutation and half by scattering in each population. This constitutes a reasonable setup in the GA since scattering or mutation alone is ineffective at all. By specifying the population type to Bit String, each density element will conserve its binary representation during mutation.

Once again, in optimization problems the initial population plays an important role in drawing a general view for the final solution and speeding its convergence (Figure 12). This special initialization of the problem speeds up the convergence, where it reached the optimal solution after 12 generations. Although, this work cannot be directly compared to previous bit-array methods (different applications), surely it is more efficient due to the representation form, the appropriate number of FE equations solved for each individual, and the physical generation of the initial population. Finally, we obtain the following mass representation regarding its conserved external dimensions (rectangle 8\*6). It

is represented with the refined mesh of the optimal domain (

Figure 13).

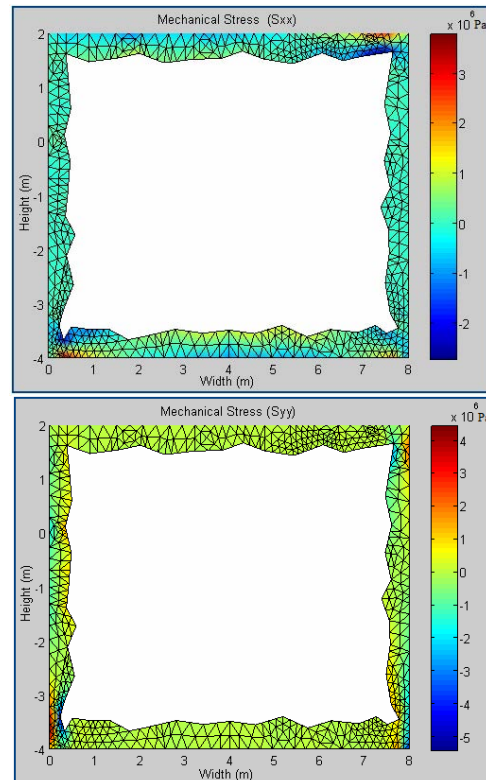


Figure 13 Mechanical stresses  $\sigma_x$  (upper) and  $\sigma_y$  (lower)

### 6- Shape Optimization Using Variable Number of Points

In this section, we introduce a variable number of points which create a valid domain where their corresponding coordinates represent the variables of the optimization problem. We search for the optimum shape composed from the optimum number of points. The update of the number of points is controlled by the relative error of the objective function. If the relative error between the objective functions of the shape created by the actual number of points and that created by the previous number of points is greater than  $\epsilon$  (value specified by the designer), then the number of points must be updated. In other words, minimize the objective function by additional points until no improvements are achieved. These points are not selected from the meshed domain, but they themselves create this new domain. Similarly, to the topology problem, a structural domain is defined by the variable points in each iteration and then a refined mesh is generated for FE analysis.

Therefore, we do not suffer from the problem of elements distortion, since the mesh is generated after indicating the points coordinates. In a shape optimization problem, the shape of a structure is changed in each iteration during the optimization process. In this case, a fixed finite element mesh is no longer appropriate. The finite element mesh should be updated in each iteration for the new shape, loading conditions. Similarly to the mesh procedure used in the topology problem, we use two different meshes one for geometrical computations and another refined one for FE computations. Also, the size of the FE problem is varying in each iteration due to the appropriate demand for each shape.

In optimization it is very important to initialize with a significant initial solution since it plays an important role in drawing a general view for the final solution and yielding to speed its convergence toward the optimal solution; therefore the  $n$  points must create an initial valid domain and not just a set of arbitrary points.

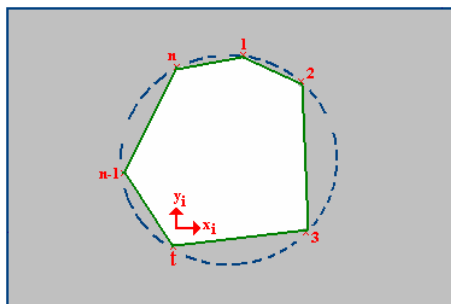


Figure 14 Initialization of a valid domain

There are two different ways to treat this problem: the first one is based on initialization of the geometric domain for every new number of points  $n$ , where the other is based on benefiting from the previous results and proceeding ahead by introducing new points to the obtained shape for the new value of  $n$ . For the first one, in order to guarantee the existence of analyzable structures in the initial solution, and especially when considering high values of  $n$ , a mathematical trick is implemented. It is based on selecting the  $n$  points on a fictitious circle (Figure 14), where each point holds a value between  $[0, 2\pi]$ .  $l = f(0, 2\pi)$ , where  $f$  represents a function giving spaced points in this interval consequently,  $\Rightarrow l_{t-1} < l_t < l_{t+1}$ , then

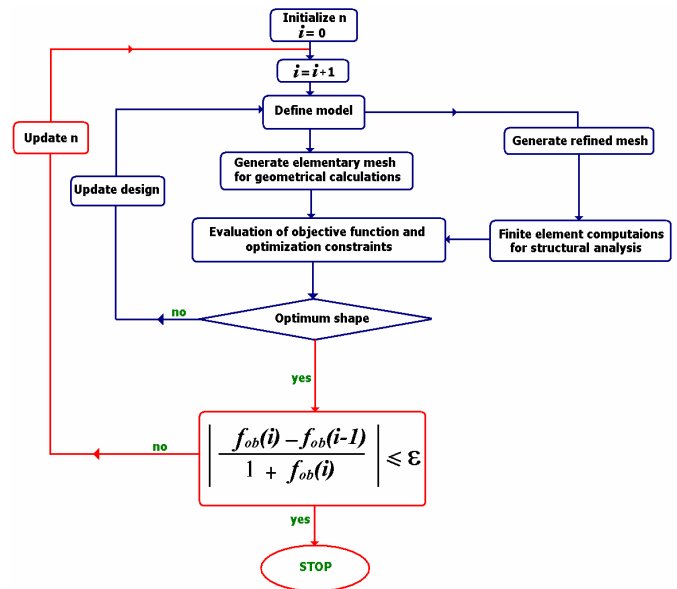
$$x_t = r \times \cos(l)$$

$$y_t = r \times \sin(l), \quad t = 1, \dots, n$$

Moreover, these points are connected by straight lines in an ordered manner:

$$1 \rightarrow 2 \rightarrow \dots \rightarrow t \dots \rightarrow n-1 \rightarrow n \rightarrow 1$$

After, assembling the polygon of  $n$  sides, the problem is treated in a similar manner to other optimization problems.



The basic algorithm of the shape optimization can be summarized in the following steps:

- 1-Initialize the number of points (3 or 4), and set  $i=0$
- 2-Define the new geometrical shape (rectangle including the void domain).
- 3-Generate an elementary mesh for the geometrical computations (objective function, floating and stability constraints)
- 4-Generate a refined mesh for the new geometrical domain.
- 5-Carry out the FE analysis
- 6-Evaluation of optimization constraints (SQP method)
- 7-If optimum shape for the considered value of  $n$  is obtained, check the objective test with the preceding number of points ( $f_{ob}(0)$ =weight of filled design domain to guarantee a correct initialization). If not, update the design with the same number of variable points. Finally, after the optimum shape is obtained for a considered number of points, and the test on the objective function is not satisfied, update the value of  $n$ .

Therefore, we confirm obtaining the optimum shape for each value of  $n$ , and then the values of  $n$  are updated until its optimum value is attained. The value of  $n$  can be indicated by the designer himself or can be generated through an

algorithm. For our case, we chose (n=4,5,7,11,15,20,25).

### 6.1 Objective function

The objective function can be directly expressed in terms of the numerical method as follows:

$$f_{ob}(x_i, y_i) = \rho_m \sum_{it=1}^{nt} A_{it}$$

where  $A_{it}$  corresponds to the area of each triangle in the meshed domain; and the index  $it$  corresponds to the number of the triangle, where it varies from 1 till the total number of triangles  $nt$ .

### 6.2 Floating constraint

The floating constraint can be expressed as follows: (transform the volume notations into surface notations per 1m length).

$$C_1(x_i, y_i) = \Sigma A_{it} - S_T \frac{\rho_e}{\rho_m} \leq 0$$

### 6.3 Stability constraint

Similarly to the objective function, the coordinates of the centre of gravity are expressed in terms of the centres of gravity of the meshing triangles:

$$x_g = \frac{\sum_{it=1}^{nt} A_{it} \times x_{it}}{\sum_{it=1}^{nt} A_{it}} \quad \text{and} \quad y_g = \frac{\sum_{it=1}^{nt} A_{it} \times y_{it}}{\sum_{it=1}^{nt} A_{it}}$$

where  $x_{it}$  and  $y_{it}$  are the coordinates of the centre of gravity of each triangle. Then, the relevant horizontal stability constraint ( $x_g = D/2$ ) is written as follows:

$$C_2(x_i, y_i) = \frac{\sum_{it=1}^{nt} A_{it} \times x_{it}}{\sum_{it=1}^{nt} A_{it}} - \frac{D}{2} = 0$$

### 6.4 Application and results

Considering different values for the variable  $n$ , it is very logical to terminate with such results (Figure 15). That is, the increase in the number of points representing the geometrical domain will yield to a decrease in the objective function until a certain limiting value where no improvement can be achieved after it. Moreover, introducing additional points to the obtained results from a previous  $n$  (benefit from the results of each  $n$ ), have

ameliorated the values of the objective function in comparison to those obtained by re-initializing the problem for each  $n$  (Figure 15).

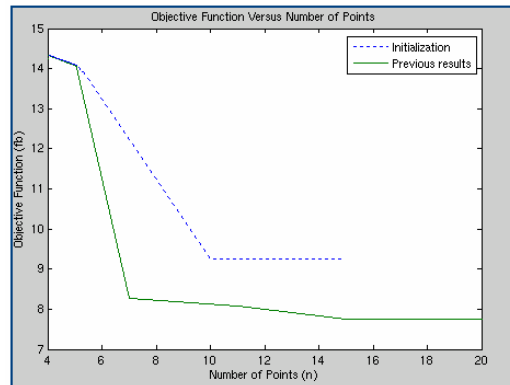


Figure 15 Variation of objective function versus n

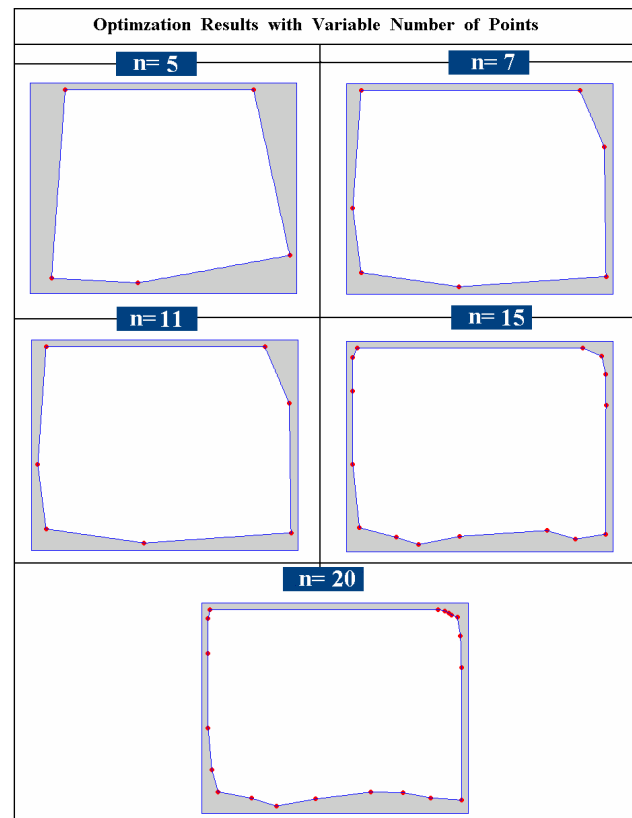


Figure 16 Optimization with variable number of points

Considering the optimization results (

Figure 16), it is obvious to start with the 4 or 5 points solution and then to go forward until no shape improvement is noticed or obtained. In consequence, when moving from 5 points to 7,11,15,20 (

Figure 16) there is a visible amelioration in the shape and the weight, where the locations of these points are also plotted on the same figures in order to understand the behaviour or the movement of

these variables during the optimization process. But, this optimization method does not comprise an infinite number of solutions for the shape improvement; it is a deterministic optimization where after a certain number of points no shape improvement can be achieved and hence we can say that an optimal solution is found. Finally, it is good to expose the optimal shape (n=20) and its relevant mechanical stresses distribution inside the studied domain (Figure 17).

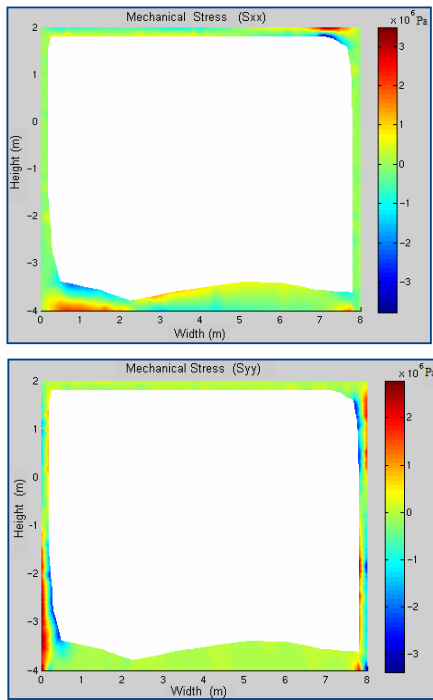


Figure 17 Mechanical stresses  $\sigma_x$  (first) and  $\sigma_y$  (second)

### 7-Discussions and Conclusions

This work constitutes a comprehensive study in optimizing floating breakwaters, since it begins with modelling sea waves and determining its induced pressures on structures. Second, it considered the physical constraints such as floating and stability, and also the essential constraint in structures design represented by limitations on the mechanical stresses. Finally, all the preceding constraints are assembled in an optimization problem solved by three different methods. A comparison between these methods is introduced and based on the numerical values of the objective function and the cost calculation of these methods (Table 1).

$f_{ob}/\rho_m$	11.278 m <sup>2</sup>	12.1 m <sup>2</sup>	7.76 m <sup>2</sup>
$f-count$	173	11800	819

The third method proved its robustness. It produced the best objective function since the  $n$  points can freely move in the domain without any restrictions. The first method produce a bigger objective function when compared with the previous due to its predefined geometry that cannot be altered but only vary in dimensions. On the other side, method 2 as we have commented on it earlier cannot be compared to values of shape optimization rather than it is very effective in problems with irregular geometries and domain helping to draw an initial image on the mass distribution in this structure to be passed later to a shape optimization problem to ameliorate its shape and weight. But, what is interesting in this method is the new type of representation in topology problems summarized by the triangular mesh, which holds up many advantages when compared to the previous (rectangular and voronoi). Also, the variable F.E problem size is a new idea in topology problems yielding to reduce the entire consumable time. It will be very efficient when solving for 3D floating breakwaters. Moreover, it is very logical to obtain higher mechanical stresses in the third method (Fig. 16) when compared to those compared in the first one (Fig. 7) and this is due to difference in the obtained volume for the two cases; where surely the structure with less material volume will hold up higher mechanical stresses. But in the second one (Fig.12), high mechanical stresses are caused by the rough surfaces.

Finally, the third method seems to have an accepted computational cost (Table 1) in comparison with the others and also due to the optimal shapes and results derived from it. In fact, it is not only a problem of volume consuming, but also a structural advantage where the floating breakwater is working approximately in the same stress domain (Figure 7); while in the case of a fixed bottom breakwater (filled material breakwater) the stress domain is largely varying between the points inside the breakwater. This is an additional advantage for the floating breakwater, since the more the inside points are working on closer stresses values the more the extended life of the structure is expected and vice versa.

<b>Table 1</b>	<b>Method 1</b>	<b>Method 2</b>	<b>Method 3</b>
----------------	-----------------	-----------------	-----------------

## References

- [1]. Boissonnat J.D, and Yvinec M., *Algorithmic geometry*. Cambridge University Press, UK, 1998.
- [2]. Cappello. F, Mancuso, A genetic algorithm for combined topology and shape optimisations, *Computer-Aided Design*, Vol 35, 2002, 761-769
- [3]. Cho S., Jung H., Design sensitivity analysis and topology optimization of displacement-loaded non-linear structures, *Computer Methods in Applied Mechanics and Engineering*, Vol. 192, 2003, 359-2553.
- [4]. Drimer, N., Agnon, Y., Stiassnie, 1992. A simplified analytical model for a floating breakwater in water of finite depth. *Applied Ocean Research* Vol. 14,1992, 33–41.
- [5]. Elchahal. G., Younes. R., Lafon. P., (2006) "Shape and Material Optimization of a 2D Vertical Floating Breakwater", *WSEAS transaction on Fluid Mechanics*, Vol 1, 2006, 355-363.
- [6]. Fanjoy D.W., Crossley W.A., Topology design of planar cross-sections with a genetic algorithm: Part 1–Overcoming the obstacles, *Engineering Optimisation* Vol 34 (1), 2002, 1–12.
- [7]. Garrigues. J, *Statique des Solides élastiques en petites déformations*, Ecole Supérieure de Mécanique de Marseille, 2001.
- [8]. Gesraha. M, Analysis of [] shaped floating breakwater in oblique waves: Impervious rigid wave boards. *Applied Ocean Research*, Vol 28, 2006, 327-338.
- [9]. Hamda H., Jouve F., Lutton E., Schoenauer M., Sebag M., Compact unstructured representations for evolutionary design, *Applied Intelligence*, Vol 16 (2), 2002, 139–155.
- [10]. Jakiela M.J., Chapman C., Duda J., Adewuya A., Saitou K., Continuum structural topology design with genetic algorithms, *Computer Methods in Applied Mechanics and Engineering*, Vol 186 (2–4), 2000, 339–356.
- [11]. Lee. J & Cho. W., Hydrodynamic analysis of wave interactions with a moored floating breakwater using the element-free Galerkin method, *Canadian Journal of Civil Engineering*, Vol 30, 2003, 720–733.
- [12]. Loukogeorgaki E. and Angelides D. Stiffness of mooring lines and performance of floating breakwater in three dimensions. *Applied Ocean Research*, Vol 27, 2005, 187-208.
- [13]. Ryu. Y.S, Park. K.B, Kim. T.B., and Na W.B, Optimum Design of Composite Breakwater with Metropolis GA, *6<sup>th</sup> World Congresses of Structural and Multidisciplinary Optimization* - Rio de Janeiro, 30 May - 03 June 2005, Brazil
- [14]. Schoenauer M., Shape representations and evolutionary schemes, in: *Evolutionary Programming: Proceedings of the Fifth Annual Conference on Evolutionary Programming*, San Diego, USA, 1996, 121–129.
- [15]. Shen Y.M, Zheng Y.H, You Y.G. On the radiation and diffraction of linear water waves by a rectangular structure over a sill. Part I Infinite domain of finite water depth. *Ocean Engineering*, Vol 32, 2005, 1073-1097.
- [16]. Sigmund O., A 99 line topology optimization code written in Matlab, *Structural. Multidisciplinary Optimization*, Vol 21, 2001, 120-127.
- [17]. Tanskanen P., The evolutionary structural optimization method: Theoretical aspects, *Computer Methods in Applied Mechanics and Engineering*, Vol 191, 2002, (47-48), 5485-5498.
- [18]. Uysala H, Gula R., Uzmanb U., Optimum shape design of shell structures, *Engineering and Structures*, Vol 29, 2007, 80–87.
- [19]. Wang S.Y, Tai .K, Structural topology design optimization using Genetic Algorithms with a bit array representation, *Computer Methods in Applied Mechanics and Engineering*, Vol 194, 2005, 3749-3770.
- [20]. Williams, A.N., Froude–Krylov force coefficients for bodies of rectangular section in the vicinity of the free-surface and sea-bed. *Ocean Engineering*, Vol 21 (7),1994, 663–682.
- [21]. Williams, A.N., and Abul-Azm A.G. Dual Pontoon Floating Breakwater. *Ocean Engineering*, Vol 24 (5), 1997, 465-478.
- [22]. Williams, A.N., Lee, H.S., Huang, Z., Floating pontoon breakwaters. *Ocean Engineering*, Vol 27, 2000, 221–240.